Ps formation in the laser-assisted e^+-He collision

Li Shu-Min
Chinese Center of Advanced Science and Technology (World Laboratory), P.O. Box 8730, Beijing 100080, People's Republic of China and Modern Physics Department, University of Science and Technology of China, Hefei, Anhui 230026, People's Republic of China

Chen Ji
Modern Physics Department, University of Science and Technology of China, Hefei, Anhui 230026, People's Republic of China

Zhou Jian-Ge
Chinese Center of Advanced Science and Technology (World Laboratory), P.O. Box 8730, Beijing 100080, People's Republic of China and Modern Physics Department, University of Science and Technology of China, Hefei, Anhui 230026, People's Republic of China

Yin Hong-Jun
Modern Physics Department, University of Science and Technology of China, Hefei, Anhui 230026, People's Republic of China
(Received 5 February 1992)

Using the first Born approximation and the $\mathbf{A}\cdot\mathbf{p}$ gauge, the Ps formation in a laser-assisted positron-helium collision is studied. In reducing the S matrix, we have developed an exponential-parameter integration technique which causes the laser-modified scattering amplitude to be reduced from nine-dimensional infinite integrals to one-dimensional finite ones without a singularity. Our results indicate that when the laser electric vector is parallel to the incident momentum, the integral cross section for Ps formation decreases, but when the electric vector is perpendicular to the incident momentum, the integral cross section increases. These results are quite different from that for an atomic-hydrogen target.

PACS number(s): 34.50.Rk, 34.70.+e, 32.80.Wr, 02.70.−c

I. INTRODUCTION

With the development of positron physics, now it is possible to measure the positronium formation cross sections in the positron-atom collisions process in the laboratory [1,2], and the accuracy has steadily improved. Some authors also studied these reaction from a theoretical perspective [1,3,4]. They found that the theory agrees well with experiment at the relatively low impact energy range.

In a recent paper of ours [5], a treatment of laser-assisted rearrangement collision between a positron and atomic hydrogen was proposed, which is based on the $\mathbf{A}\cdot\mathbf{p}$ gauge in solving the dressed states of atoms. This allows the consideration of a strong laser field, provided that the electric-field strength $\mathcal{E}_0$ remains small with respect to the atomic unit of field strength, namely, $\mathcal{E}_0 \ll 5.14\times10^9\ \mathrm{V\,cm^{-1}}$.

In the present article, we intend to extend our previous treatment of an atomic-hydrogen target to the laser-assisted e^+-He charge-transfer process. In reducing the S matrix, a technique of integral reduction, the exponential-parameter integration technique, is developed. A comparison of the results with that for the atomic-hydrogen target is also made.

The paper is arranged as follows: In Sec. II, we give the general theory. Some results are displayed and discussed in Sec. III. Section IV is a conclusion. Finally, in the Appendix, we detail the reduction of a typical integral in the S matrix, which concerns the dressing effect of the laser.

II. THEORY

We assume that the laser field is monochromatic, linearly polarized, and of low frequency

$$\mathbf{A}=\mathbf{A}_0\cos\omega t=\frac{c}{\omega}\mathcal{E}_0\cos\omega t, \tag{2.1}$$

where $\mathcal{E}_0$ is the electric vector. The rearrangement collision

$$e^+ + \mathrm{He}\rightarrow \mathrm{Ps}+\mathrm{He}^+ \tag{2.2}$$

is embedded in this laser field as shown in Fig. 1. $\mathbf{r}_0$ is the position vector of the positron, $\mathbf{r}_1$ and $\mathbf{r}_2$ are the position vectors of the two electrons of helium, respectively. The target nucleus is supposed to be at rest at the origin.

A. Dressed wave functions

For the initial channel, the Hamiltonian of the positron-helium system in the presence of the laser field

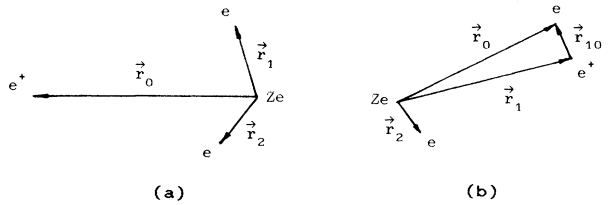

FIG. 1. The laser-assisted reaction $e^+ + \mathrm{He}\rightarrow \mathrm{Ps}+\mathrm{He}^+$ (a) before collision, (b) after collision.

may be decomposed into three parts (in atomic units)

$$H = H_{e^+} + H_{\mathrm{He}} + V_I \tag{2.3}$$

in which

$$H_{e^+} = \frac{1}{2}\left[\mathbf{p}_0 - \frac{1}{c}\mathbf{A}\right]^2, \tag{2.4}$$

$$H_{\mathrm{He}} = \frac{1}{2}\left[\mathbf{p}_1 + \frac{1}{c}\mathbf{A}\right]^2 + \frac{1}{2}\left[\mathbf{p}_2 + \frac{1}{c}\mathbf{A}\right]^2 - \frac{2}{r_1} - \frac{2}{r_2} + \frac{1}{r_{12}}, \tag{2.5}$$

$$V_I = \frac{2}{r_0} - \frac{1}{r_{10}} - \frac{1}{r_{20}}. \tag{2.6}$$

The initial wave function is

$$\Psi_I(\mathbf{r}_0,\mathbf{r}_1,t) = \chi_I(\mathbf{r}_0,t)\psi_0^{\mathrm{He}}(\mathbf{r}_1,\mathbf{r}_2,t), \tag{2.7}$$

where $\chi_I(\mathbf{r}_0,t)$ is the laser-assisted state of the incident positron $\psi_0^{\mathrm{He}}(\mathbf{r}_1,\mathbf{r}_2,t)$ is the dressed ground state of helium. The positron state χ_I is given by the Volkov solution [6]

$$\chi_I(\mathbf{r}_0,t) = (2\pi)^{3/2}\exp[i(\mathbf{k}_I\cdot\mathbf{r}_0 + \mathbf{k}_I\cdot\boldsymbol{\alpha}_0\sin\omega t - E_I t)], \tag{2.8}$$

where $\mathbf{k}_I$ is the incident momentum, $E_I = k_I^2/2$ is the impact kinetic energy, $\alpha_0 = \mathcal{E}_0/\omega^2$. In writing the Volkov solution (2.8), *we have omitted the term involving* A^2, which is not of much importance for the range of electric-field strength we have considered. According to our preceding work [5], the dressed wave function ψ_0^{He} in Eq. (2.7) can be obtained by the first-order time-dependent perturbation theory in the $\mathbf{A}\cdot\mathbf{p}$ gauge

$$\psi_0^{\mathrm{He}}(\mathbf{r}_1,\mathbf{r}_2,t) = e^{-iW_0^{\mathrm{He}}t}\left\{\phi_0^{\mathrm{He}}(\mathbf{r}_1,\mathbf{r}_2) - \frac{1}{2}\sum_{n\,(\neq 0)}\left[\frac{e^{i\omega t}}{\omega_{n0}+\omega} + \frac{e^{-i\omega t}}{\omega_{n0}-\omega}\right]\left\langle\phi_n^{\mathrm{He}}(\mathbf{r}_1,\mathbf{r}_2)\left|\frac{1}{\omega c}\mathbf{A}_0\cdot(\mathbf{p}_1+\mathbf{p}_2)\right|\phi_0^{\mathrm{He}}(\mathbf{r}_1,\mathbf{r}_2)\right\rangle\phi_n^{\mathrm{He}}(\mathbf{r}_1,\mathbf{r}_2)\right\}, \tag{2.9}$$

where $\phi_0^{\mathrm{He}}(\mathbf{r}_1,\mathbf{r}_2)$ and $\phi_n^{\mathrm{He}}(\mathbf{r}_1,\mathbf{r}_2)$ are the ground and the nth eigenstates of helium with eigenenergies W_0^{He} and W_n^{He}, respectively, $\omega_{n0} = W_n^{\mathrm{He}} - W_0^{\mathrm{He}}$ is the atomic excitation energy. In view of the closure approximation and the fact that $\omega_{n0} \gg \omega$, Eq. (2.9) can be written as

$$\psi_0^{\mathrm{He}}(\mathbf{r}_1,\mathbf{r}_2,t) = e^{-iW_0^{\mathrm{He}}t}[\phi_0^{\mathrm{He}}(\mathbf{r}_1,\mathbf{r}_2) - \cos(\omega t)\tilde{\phi}_0^{\mathrm{He}}(\mathbf{r}_1,\mathbf{r}_2)] \tag{2.10}$$

in which $W_0^{\mathrm{He}} = -79.010$ eV, $\phi_0^{\mathrm{He}}(\mathbf{r}_1,\mathbf{r}_2)$ is the Hartree-Fock wave function of the ground state, namely [7]

$$\phi_0^{\mathrm{He}}(\mathbf{r}_1,\mathbf{r}_2) = \phi_0(\mathbf{r}_1)\phi_0(\mathbf{r}_2) \tag{2.11}$$

with

$$\phi_0(\mathbf{r}) = \frac{1}{\sqrt{4\pi}}\sum_{i=1}^{2} C_i e^{-\alpha_i r}, \tag{2.12}$$

where $C_1 = 2.605\,05$, $C_2 = 2.081\,44$, $\alpha_1 = 1.41$, and $\alpha_2 = 2.61$. In Eq. (2.10), $\tilde{\phi}_0^{\mathrm{He}}(\mathbf{r}_1,\mathbf{r}_2)$ is the term related to laser-atom interaction

$$\tilde{\phi}_0^{\mathrm{He}}(\mathbf{r}_1,\mathbf{r}_2) = \frac{1}{\omega_{\mathrm{He}}c}\mathbf{A}_0\cdot(\mathbf{p}_1+\mathbf{p}_2)\phi_0^{\mathrm{He}}(\mathbf{r}_1,\mathbf{r}_2) = \frac{1}{\omega_{\mathrm{He}}\omega}i\mathcal{E}_0\cdot\frac{1}{4\pi}\sum_{i,j=1}^{2}(\alpha_i\hat{\mathbf{r}}_1 + \alpha_j\hat{\mathbf{r}}_2) \times C_i C_j e^{-\alpha_i r_1}e^{-\alpha_j r_2}, \tag{2.13}$$

where $\omega_{\mathrm{He}} = 1.15$ a.u. is the average excitation energy of helium [8], $\hat{\mathbf{r}}_1$ and $\hat{\mathbf{r}}_2$ are the unit vectors of $\mathbf{r}_1$ and $\mathbf{r}_2$, respectively.

The Hamiltonian for the final channel is

$$H = H_{\mathrm{Ps}} + H_{\mathrm{He}^+} + V_F, \tag{2.14}$$

where

$$H_{\mathrm{Ps}} = \frac{1}{2}\left[\mathbf{p}_0 - \frac{1}{c}\mathbf{A}\right]^2 + \frac{1}{2}\left[\mathbf{p}_1 + \frac{1}{c}\mathbf{A}\right]^2 - \frac{1}{r_{10}}, \tag{2.15}$$

$$H_{\mathrm{He}^+} = \frac{1}{2}\left[\mathbf{p}_2 + \frac{1}{c}\mathbf{A}\right]^2 - \frac{2}{r_2}, \tag{2.16}$$

$$V_F = \frac{2}{r_0} - \frac{2}{r_1} - \frac{1}{r_{02}} + \frac{1}{r_{12}}. \tag{2.17}$$

The final wave function is

$$\Psi_F(\mathbf{r}_1,\mathbf{r}_2,t) = \chi_F(\mathbf{s},t)\psi_0^{\mathrm{Ps}}(\mathbf{r}_{10},t)\psi_0^{\mathrm{He}^+}(\mathbf{r}_2,t), \tag{2.18}$$

with $\mathbf{s} = (\mathbf{r}_1+\mathbf{r}_0)/2$, $\mathbf{r}_{10} = \mathbf{r}_1 - \mathbf{r}_0$. In Eq. (2.18), $\chi_F(\mathbf{s},t)$ and $\psi_0^{\mathrm{Ps}}(\mathbf{r}_{10},t)$ relate to the mass center motion and the internal state of Ps atom respectively. $\psi_0^{\mathrm{He}^+}(\mathbf{r}_2,t)$ is the dressed ground state of helium ion. As was obtained for the final state, we obtain

$$\chi_F(\mathbf{s},t) = (2\pi)^{-3/2}\exp[i(\mathbf{k}_F\cdot\mathbf{s} - E_F t)], \tag{2.19}$$

$$\psi_0^{\mathrm{Ps}}(\mathbf{r}_{10},t) = e^{-iW_0^{\mathrm{Ps}}t}[\phi_0^{\mathrm{Ps}}(\mathbf{r}_{10}) - \cos(\omega t)\tilde{\phi}_0^{\mathrm{Ps}}(\mathbf{r}_{10})], \tag{2.20}$$

where $E_F = k_F^2/4$, $W_0^{\mathrm{Ps}} = -\frac{1}{4}$ a.u. In Eq. (2.20)

$$\phi_0^{\mathrm{Ps}}(\mathbf{r}_{10}) = \frac{1}{\sqrt{8\pi}}e^{-\lambda r_{10}}, \tag{2.21}$$

$$\tilde{\phi}_0^{\mathrm{Ps}}(\mathbf{r}_{10}) = \frac{1}{\omega_{\mathrm{Ps}}\omega}i\mathcal{E}_0\cdot\lambda\hat{\mathbf{r}}_{10}\frac{1}{\sqrt{8\pi}}e^{-\lambda r_{10}}, \tag{2.22}$$

where $\lambda=\frac{1}{2}$, $\omega_{\rm Ps}=-\frac{2}{9}$ a.u. In the same way, we obtain

$$\psi_0^{\rm He^+}(\mathbf{r}_2,t)=e^{-iW_0^{\rm He^+}}[\phi_0^{\rm He^+}(\mathbf{r}_2)-\cos(\omega t)\tilde{\phi}_0^{\rm He^+}(\mathbf{r}_2)], \tag{2.23}$$

with

$$\phi_0^{\rm He^+}(\mathbf{r}_2)=\frac{1}{\sqrt{\pi}}e^{-2r_2}, \tag{2.24}$$

$$\tilde{\phi}_0^{\rm He^+}(\mathbf{r}_2)=\frac{2}{\omega_{\rm He^+}\omega}i\mathcal{E}_0\cdot\hat{\mathbf{r}}_2\frac{1}{\sqrt{\pi}}e^{-2r_2}, \tag{2.25}$$

where $W_0^{\rm He^+}=-2.0$ a.u., $\omega_{\rm He^+}=\frac{16}{9}$ a.u.

B. *S* matrix

With considering the fact that V_1 is symmetric to the exchange of $\mathbf{r}_1$ and $\mathbf{r}_2$, we may write the prior form of the S matrix for laser-assisted Ps formation in the first Born approximation

$$S_{FI}^{B_1}=-i\sqrt{2}\int_{-\infty}^{\infty}dt\langle\Psi_F|V_I|\Psi_I\rangle$$
$$=(2\pi)^{-1}i\sum_{L=-\infty}^{\infty}f_L^{B_1}\delta(E_F+W_0^{\rm Ps}+W_0^{\rm He^+}-E_I-W_0^{\rm He}+L\omega), \tag{2.26}$$

where

$$f_L^{B_1}=J_L(\mathbf{k}_I\cdot\boldsymbol{\alpha}_0)\{f_0^{B_1}(\mathbf{q}_0,\mathbf{q}_1)-(\mathbf{k}_I\cdot\boldsymbol{\alpha}_0)^{-1}L\tilde{f}_0^{B_1}(\mathbf{q}_0,\mathbf{q}_1)\}, \tag{2.27}$$

with $\mathbf{q}_0=\mathbf{k}_F/2-\mathbf{k}_I$, $\mathbf{q}_1=\mathbf{k}_F/2$. In Eq. (2.27)

$$f_0^{B_1}(\mathbf{q}_0,\mathbf{q}_1)=f^{B_1}(\phi_0^{\rm He}\to\phi_0^{\rm Ps}\phi_0^{\rm He^+}), \tag{2.28}$$

$$\tilde{f}^{B_1}(\mathbf{q}_0,\mathbf{q}_1)=f^{B_1}(\tilde{\phi}_0^{\rm He}\to\phi_0^{\rm Ps}\phi_0^{\rm He^+})+f^{B_1}(\phi_0^{H}\to\tilde{\phi}_0^{\rm Ps}\phi_0^{\rm He^+})+f^{B_1}(\phi_0^{\rm He}\to\phi_0^{\rm Ps}\tilde{\phi}_0^{\rm He^+}). \tag{2.29}$$

Each term on the right-hand sides of Eqs. (2.28) and (2.29) is the FBA amplitude corresponding to the transition process in each parenthesis. With use of the Feynman integration technique developed in our previous paper, we obtain

$$f_0^{B_1}(\mathbf{q}_0,\mathbf{q}_1)=-\frac{m_{\rm Ps}}{2\pi}\int d^3(r_0r_1)e^{-i\mathbf{q}_0\cdot\mathbf{r}_0}e^{-i\mathbf{q}_1\cdot\mathbf{r}_1}\phi_0^{\rm Ps*}(\mathbf{r}_{10})\times\phi_0^{\rm He^+*}(\mathbf{r}_2)V_I\phi_0^{\rm He}(\mathbf{r}_1,\mathbf{r}_2)$$
$$=-8\sum_{i,j}C_iC_jI_{ij} \tag{2.30}$$

with

$$I_{ij}=\frac{2}{\beta_j^3}\frac{\partial}{\partial\alpha_i}\left[\frac{\partial}{\partial\lambda}-\frac{\partial}{\partial\gamma}\right]I(\mathbf{q}_0,\gamma,\mathbf{q}_1,\alpha_i,\lambda)+\left[\frac{2}{\beta_j^3}-\frac{1}{\beta_j^2}\frac{\partial}{\partial\beta_j^2}\right]\frac{\partial^2}{\partial\alpha_i\partial\lambda}I(\mathbf{q}_0,\beta_j,\mathbf{q}_1,\alpha_i,\lambda), \tag{2.31}$$

where $\gamma=0$, $\beta_j=\alpha_j+2$, $m_{\rm Ps}=2$. I is a one-dimensional integral which has the general form [5]

$$I(\mathbf{q}_0,\beta,\mathbf{q}_1,\alpha,\lambda)=\frac{1}{8\pi^2}\int d^3(r_0r_1)\frac{e^{-i\mathbf{q}_0\cdot\mathbf{r}_0-\beta r_0}}{r_0}\frac{e^{-i\mathbf{q}_1\cdot\mathbf{r}_1-\alpha r_1}}{r_1}\frac{e^{-\lambda r_{10}}}{r_{10}}$$
$$=\int_0^1 d\xi\frac{1}{\rho[(\rho+\beta)^2+q^2]} \tag{2.32}$$

with

$$\mathbf{q}=\mathbf{q}_0+\mathbf{q}_1\xi, \tag{2.33}$$

$$\rho=[\lambda^2+(q_1^2+\alpha^2-\lambda^2)\xi-q_1^2\xi^2]^{1/2}. \tag{2.34}$$

Similarly, we obtain

$$\tilde{f}_0^{B_1}(\mathbf{q}_0,\mathbf{q}_1)=-\frac{m_{\rm Ps}}{2\pi}\int d^3(r_0r_1)e^{-i\mathbf{q}_0\cdot\mathbf{r}_0}e^{-i\mathbf{q}_1\cdot\mathbf{r}_1}\times[\tilde{\phi}_0^{\rm Ps*}(\mathbf{r}_{10})\phi_0^{\rm He^+*}(\mathbf{r}_2)V_I\phi_0^{\rm He}(\mathbf{r}_1,\mathbf{r}_2)+\phi_0^{\rm Ps*}(\mathbf{r}_{10})\tilde{\phi}_0^{\rm He^+*}(\mathbf{r}_2)V_I\phi_0^{\rm He}(\mathbf{r}_1,\mathbf{r}_2)+\phi_0^{\rm Ps*}(\mathbf{r}_{10})\phi_0^{\rm He^+*}(\mathbf{r}_2)V_I\tilde{\phi}_0^{\rm He}(\mathbf{r}_1,\mathbf{r}_2)]=-8\sum_{i,j}C_iC_j\tilde{I}_{ij}, \tag{2.35}$$

where

$$\tilde{I}_{ij}=\frac{2}{\beta_j^3}\left\{-u\frac{\partial^2}{\partial\alpha_i\partial q_{0\varepsilon}}+\left[u\frac{\partial}{\partial\alpha_i}+v_i\left[\frac{\partial}{\partial\lambda}-\frac{\partial}{\partial\gamma}\right]\right]\frac{\partial}{\partial q_{1\varepsilon}}I(\mathbf{q}_0,\gamma,\mathbf{q}_1,\alpha_i,\lambda)\right\}$$
$$+\left[\frac{2}{\beta^3}-\frac{1}{\beta^2}\frac{\partial}{\partial\beta}\right]\left[-u\frac{\partial}{\partial\alpha_i\partial q_{0\varepsilon}}+\left[u\frac{\partial}{\partial\alpha_i}+v_i\frac{\partial}{\partial\lambda}\right]\frac{\partial}{\partial q_{1\varepsilon}}I(\mathbf{q}_0,\beta_j,\mathbf{q}_1,\alpha_i,\lambda)\right]+w_j\frac{2}{\beta_j^4}\frac{\partial^2}{\partial\alpha_i\partial\lambda}J(\mathbf{q}_0,\gamma,\mathbf{q}_1,\alpha_i,\lambda)$$
$$-w_j\left[\frac{2}{\beta_j^4}-\frac{2}{\beta_j^3}\frac{\partial}{\partial\beta_j}+\frac{1}{\beta_j^2}\frac{\partial}{\partial\beta_j^2}\right]\frac{\partial^2}{\partial\alpha_i\partial\lambda}J(\mathbf{q}_0,\gamma,\mathbf{q}_1,\alpha_i,\lambda)-u\frac{2}{\beta_j^3}T(\mathbf{q}_0,\lambda,\mathbf{q}_1+\mathbf{q}_0,\alpha_i) \tag{2.36}$$

with

$$u=-\frac{\lambda\mathcal{E}_0}{\omega\omega_{\rm Ps}}, \tag{2.37}$$

$$v_i=\frac{\alpha_i\mathcal{E}_0}{\omega\omega_{\rm He}}, \tag{2.38}$$

$$w_j=\frac{\mathcal{E}_0}{\omega}\left[\frac{\alpha_j}{\omega_{\rm He}}-\frac{2}{\omega_{\rm He^+}}\right]. \tag{2.39}$$

J is another numerical integral

$$J(\mathbf{q}_0,\beta,\mathbf{q}_1,\alpha,\lambda)=\frac{1}{8\pi^2 i}\int d^3(r_0 r_1)\frac{e^{-i\mathbf{q}_0\cdot\mathbf{r}_0-\beta r_0}}{r_0^2}\hat{\boldsymbol{\varepsilon}}\cdot\hat{\mathbf{r}}_0 \times\frac{e^{-i\mathbf{q}_1\cdot\mathbf{r}_1-\alpha r_1}}{r_1}\frac{e^{-\lambda r_{10}}}{r_{10}} =\int_0^1 d\xi\frac{q_\varepsilon}{q^3}\frac{\rho+\beta}{\rho}\left[\frac{\pi}{2}-\arctan\frac{q+\beta}{q}\right] \tag{2.40}$$

in which $\hat{\boldsymbol{\varepsilon}}$ is the unit vector of $\mathscr{E}_0$, $\mathbf{q}$ and ρ are given by Eqs. (2.33) and (2.34), respectively. The proof of Eq. (2.40) appears in the Appendix. T is an analytical expression [5]

$$T(\mathbf{q}_0,\beta,\mathbf{q}_1,\alpha)=\frac{1}{8\pi^2 i}\int d^2(r_0 r_1)\frac{e^{-i\mathbf{q}_0\cdot\mathbf{r}_0-\beta r_0}}{r_0}\hat{\boldsymbol{\varepsilon}}\cdot\hat{\mathbf{r}}_0 e^{-i\mathbf{q}_1\cdot\mathbf{r}_0-\alpha r_1} =\frac{4\alpha}{(\alpha^2+q_1^2)^2}\frac{q_{0\varepsilon}}{q_0^3}\left[\frac{\beta q_0}{\beta^2+q_0^2}-\arctan\frac{q_0}{\beta}\right]. \tag{2.41}$$

Substituting Eqs. (2.30) and (2.35) into Eq. (2.27), we finally obtain

$$f_L^{B_1}=-8\sqrt{2}J_l(\mathbf{k}_I\cdot\boldsymbol{\alpha}_0)\times\sum_{i,j}C_i C_j\left[\mathcal{I}_{ij}+LU\frac{2}{\beta_j^3}T(\mathbf{q}_0,\lambda,\mathbf{q}_1+\mathbf{q}_0,\alpha_i)\right] \tag{2.42}$$

in which

$$\begin{aligned}\mathcal{I}_{ij}=&\frac{2}{\beta_j^3}\left\{\frac{\partial^2}{\partial\alpha_i\partial\lambda}-L\left[-U\frac{\partial^2}{\partial\alpha_i\partial q_{0\varepsilon}}+\left[U\frac{\partial}{\partial\alpha_i}-V_i\frac{\partial}{\partial\lambda}\right]\frac{\partial}{\partial q_{1\varepsilon}}\right]\right\}I(\mathbf{q}_0,\gamma,\mathbf{q}_1,\alpha_i,\lambda)\\&-\frac{2}{\beta_j^3}\left[\frac{\partial}{\partial\alpha_i}-LV_i\frac{\partial}{\partial q_{1\varepsilon}}\right]\frac{\partial}{\partial\gamma}I(\mathbf{q}_0,\gamma,\mathbf{q}_1,\alpha_i,\lambda)-LW_j\frac{2}{\beta_j^4}\frac{\partial^2}{\partial\alpha_i\partial\lambda}J(\mathbf{q}_0,\gamma,\mathbf{q}_1,\alpha_i,\lambda)\\&+\left[\frac{2}{\beta_j^3}-\frac{1}{\beta_j^2}\frac{\partial}{\partial\beta_j}\right]\left\{\frac{\partial^2}{\partial\alpha_i\partial\lambda}-L\left[-U\frac{\partial^2}{\partial\alpha_i\partial q_{0\varepsilon}}+\left[U\frac{\partial}{\partial\alpha_i}+V_i\frac{\partial}{\partial\lambda}\right]\frac{\partial}{\partial q_{1\varepsilon}}\right]\right\}I(\mathbf{q}_0,\beta_j,\mathbf{q}_1,\alpha_i,\lambda)\\&+LW_j\left[\frac{2}{\beta_j^4}-\frac{2}{\beta_j^3}\frac{\partial}{\partial\beta_j}+\frac{1}{\beta_j^2}\frac{\partial}{\partial\beta_j^2}\right]\frac{\partial^2}{\partial\alpha_i\partial\lambda}J(\mathbf{q}_0,\beta_j,\mathbf{q}_1,\alpha_i,\lambda)\end{aligned} \tag{2.43}$$

with

$$U=-\frac{\omega}{\omega_{\mathrm{Ps}}}\frac{\lambda}{k_I\cos\Theta}, \tag{2.44}$$

$$V_i=\frac{\omega}{\omega_{\mathrm{He}}}\frac{\alpha_i}{k_I\cos\Theta}, \tag{2.45}$$

$$W_j=\frac{\omega}{k_I\cos\Theta}\left[\frac{\alpha_j}{\omega_{\mathrm{He}}}-\frac{2}{\omega_{\mathrm{He}^+}}\right]. \tag{2.46}$$

Θ is the angle between $\mathscr{E}_0$ and $\mathbf{k}_I$.

III. RESULTS AND DISCUSSION

For the reason of brevity, we only present some typical results here for discussion. The framework is shown in

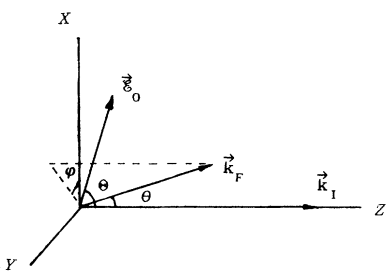

FIG. 2. The framework.

Fig. 2. We choose the Z axis along the direction of incident momentum $\mathbf{k}_I$, the electric vector $\mathscr{E}_0$ being in the ZX plane.

A. Differential cross sections

Using Eq. (2.42), we may evaluate the individual differential cross sections with the transfer of L photons

$$\frac{d\sigma_L^{B_1}}{d\Omega}=\frac{v_F}{v_I}|f_L^{B_1}|^2=\frac{1}{2}\frac{k_F}{k_I}|f_L^{B_1}|^2, \tag{3.1}$$

where $v_I=k_I$, $v_F=k_F/2$ are the velocities of e^+ and the Ps atom, respectively. Summing over all the possible L, we gain

$$\frac{d\sigma^{B_1}}{d\Omega}=\sum_{L=-\infty}^{\infty}\frac{d\sigma_L^{B_1}}{d\Omega}=\frac{1}{2}\sum_{L=-\infty}^{\infty}\frac{k_F}{k_I}|f_L^{B_1}|^2. \tag{3.2}$$

In Fig. 3, we give the differential cross sections as functions of the scattering angle θ for $\mathscr{E}_0\|\mathbf{k}_I$, $\mathscr{E}_0=1.0\times10^8$ V cm^{-1}, $\hbar\omega=1.0$ eV, and $E_I=50.0$ eV. Figure 3(a) displays the individual cross sections with L photons transferred. Because the cross section for scattering system absorbing one photon ($L=1$) is nearly identical to that for emitting one photon ($L=-1$), in the figure only one curve of them is presented. Figure 3(b) is the summa-

tion cross section over all possible L ($-50\sim50$). Unlike the result for the atomic-hydrogen target [5], for helium, the summation cross section is not always enhanced throughout all the scattering angle region.

Figure 4 is the case for $\mathcal{E}_0\perp\mathbf{k}_1$, $\varphi=0°$. The cross section is lowered at small angle but promoted at a large angle.

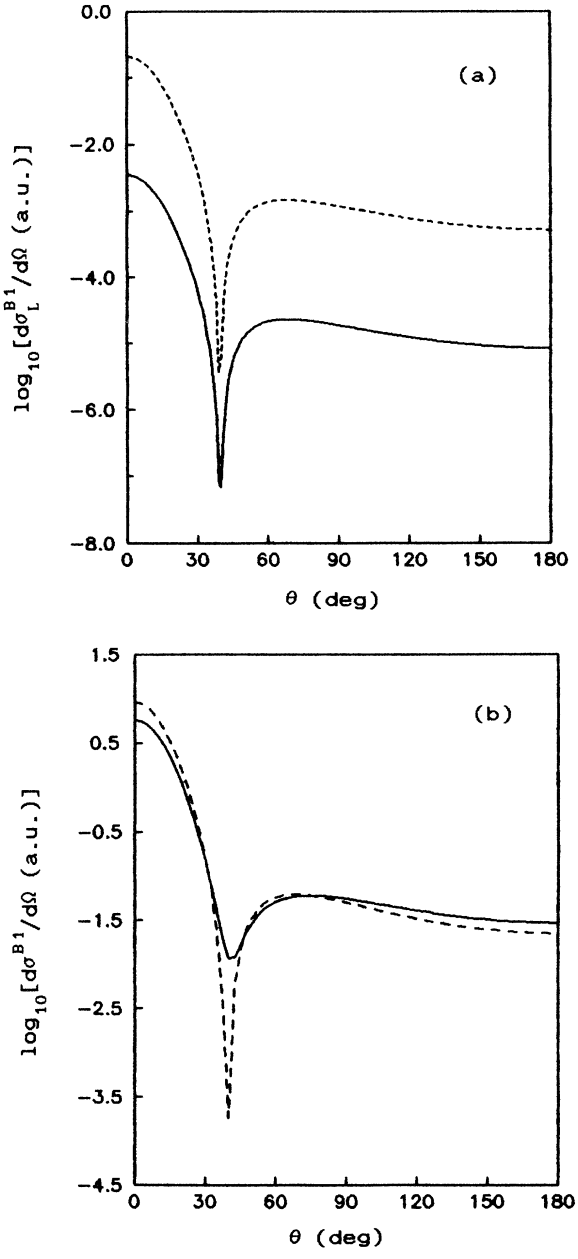

FIG. 3. The differential cross sections of the laser-assisted $e^+\rightarrow$He$\rightarrow$Ps+He^+ reaction for $\mathcal{E}_0\|\mathbf{k}_I$, $\mathcal{E}_0=1.0\times10^8$ V cm^{-1}, $\hbar\omega=1.0$ eV, $E_I=50.0$ eV. (a) Each individual differential cross section with L photons transferred between the scattering system and the laser field. ——, $L=0$ (no photon exchanged); — — —, $L=1$ (system releases one photon). (b) Summation differential cross section over all possible L. ——, laser presented; — — —, laser free.

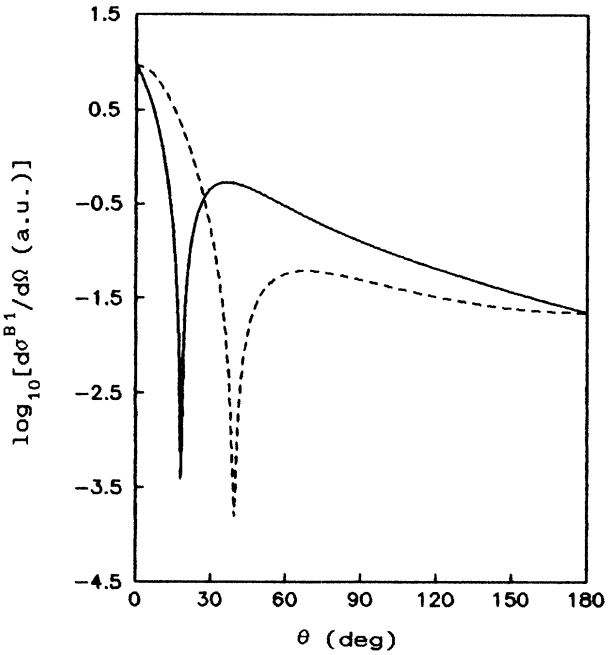

FIG. 4. Same as Fig. 3, but $\mathcal{E}_0\perp\mathbf{k}_I$, $\varphi=0°$.

Figure 5 shows the cross section as a function of the azimuth angle φ for $\mathcal{E}_0\perp\mathbf{k}_I$, $\theta=10°$. The curve is symmetric to $\theta=180°$ and approaches its maximum at this angle.

Figure 6 exhibits the differential cross sections as functions of the impact energy for $\mathcal{E}_0\|\mathbf{k}_I$, $\theta=10°$, $\mathcal{E}_0=1.0\times10^8$ V cm^{-1} and $\hbar\omega=1.0$ eV. In Figure 6(a), the individual differential cross sections have oscillating behavior which originates from the Bessel function of Eq. (2.27). The summation differential cross section shown in Fig. 6(b) is quite different from that for the atomic-hydrogen target. At lower energy the curve is sawtooth-like, and there part of it is under the cross section for laser free. This is mainly attributed to the special distribution of the electron cloud of helium.

Figure 7 is the same as Fig. 6, but for $\mathcal{E}_0\perp\mathbf{k}_I$, $\varphi=0°$.

Figure 8 reflects the relation between the differential cross sections and the amplitude of the laser field for $\mathcal{E}_0\|\mathbf{k}_I$, $\theta=10°$, $\hbar\omega=1.0$ eV, and $E_I=50.0$ eV. In Figs. 8(a) and 8(b) we give the individual cross sections and the summation cross section, respectively. Contrary to the individual cross section for atomic hydrogen target, the summation cross section is a decreasing function of $\mathcal{E}_0$.

Figure 9 is the result for $\mathcal{E}_0\perp\mathbf{k}_I$, $\theta=10°$, $\varphi=0°$. The curve also drops with decreasing $\mathcal{E}_0$, but more rapidly.

Figures 10 and 11 describe the relationship between the differential cross sections and laser frequency for $\theta=10°$, $\varphi=10°$, $\mathcal{E}_0=1.0\times10^7$ V cm^{-1}, and $E_I=50.0$ eV. In contrast to the results for the atomic hydrogen target, the laser-modified cross sections are increasing functions of $\hbar\omega$ (curves for individual cross sections are not presented here). In both geometries, the result for $\mathcal{E}_0\|\mathbf{k}_I$ (Fig. 10) is more sensitive than that for $\mathcal{E}_0\perp\mathbf{k}_I$ (Fig. 11), because the

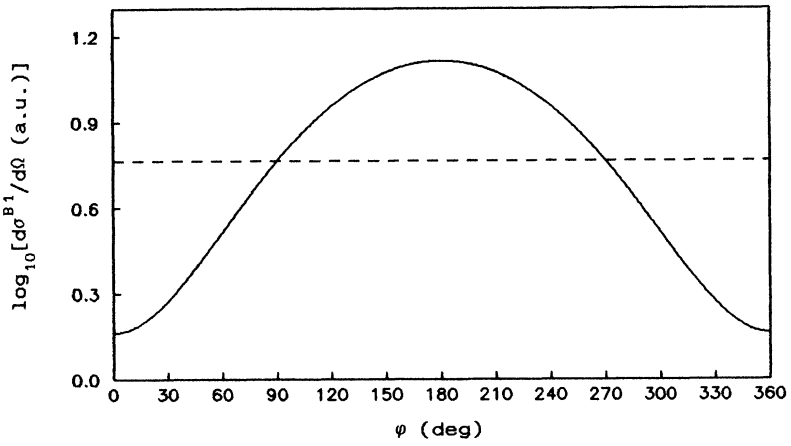

FIG. 5. Differential cross sections as functions of azimuth angle for $\mathcal{E}_0 \perp \mathbf{k}_I$, $\theta = 10°$.

former is concerning with $\mathcal{E}_0/\omega$ and $\mathcal{E}_0/\omega^2$ [see Eqs. (2.13), (2.22), (2.25), and (2.8)], but the later only concerns with $\mathcal{E}_0/\omega$.

Figure 12 demonstrates differential cross sections as functions of the laser polarization direction for $\theta = 10°$, $\varphi = 0°$, $\mathcal{E}_0 = 1.0 \times 10^8$ V cm^{-1}, $\hbar\omega = 1.0$ eV and $E_I = 50.0$ eV. The cross sections are periodic functions of Θ with a period 180°. At about $\theta = 70°$ and 250°, the summed cross section approaches its maximum.

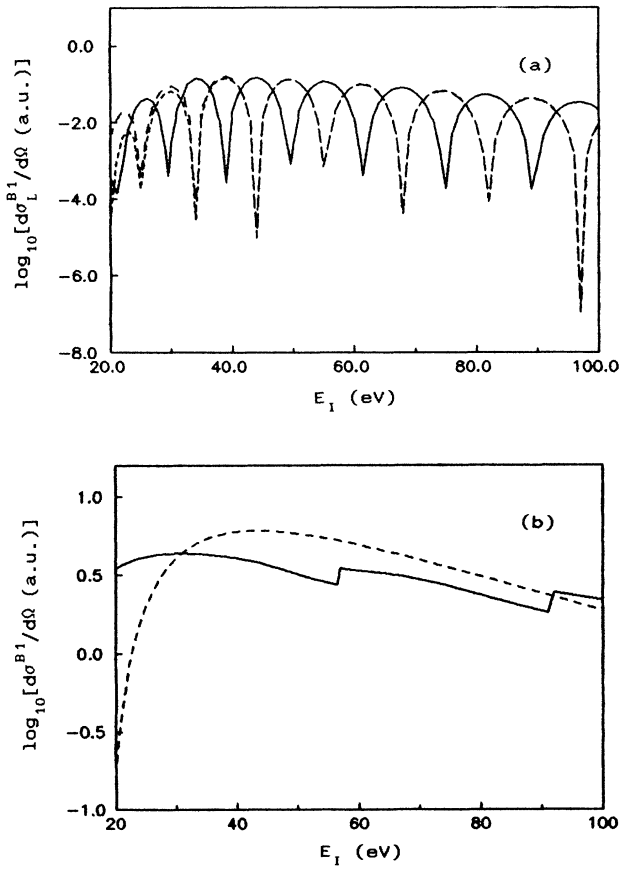

FIG. 6. The differential cross sections as functions of impact energy for $\mathcal{E}_0 \| \mathbf{k}_I$, $\theta = 10°$, $\mathcal{E}_0 = 1.0 \times 10^8$ V cm^{-1}, $\hbar\omega = 1.0$ eV. (a) Individual cross sections; ——, $L = 0$; — — —, $L = 1$; ··· ··· ···, $L = -1$. (b) Summation cross section. ——, laser presented; — — —, laser free.

B. Integral cross sections

Integrating Eq. (3.2) over all scattering angle yields the integral cross sections for Ps formation

$$\sigma_t^{B_1} = \int d\Omega \frac{d\sigma^{B_1}}{d\Omega} = \int r^2 dr \sin\theta \, d\theta \, d\varphi \frac{d\sigma^{B_1}}{d\Omega} . \quad (3.3)$$

Figure 13 depicts the integral cross sections for Ps formation as functions of impact energy for $\mathcal{E}_0 = 1.0 \times 10^8$ V cm^{-1}, $\hbar\omega = 1.0$ eV. For $\mathcal{E}_0 \| \mathbf{k}_I$ (curve I), part of the laser-modified cross section is under that for a laser-free state. This may be illustrated in Fig. 14: For the ground states of the He atom and the He^+ ion, each nucleus binds its electrons tightly. The laser influence on them is insignificant, so the dressed wave function for each of them may be substituted approximately by the corresponding state for a laser-free state. The laser mainly changes the states of the incident positron and the Ps atom. After one electron of the He atom is captured away by the positron, the remaining He^+ is a positively charged atomic core, which attracts the electron in the Ps

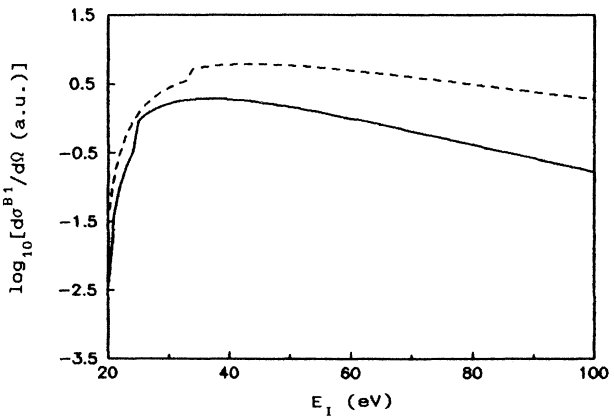

FIG. 7. Same as Fig. 6, but $\mathcal{E}_0 \perp \mathbf{k}_I$, $\theta = 10°$, $\varphi = 0°$.

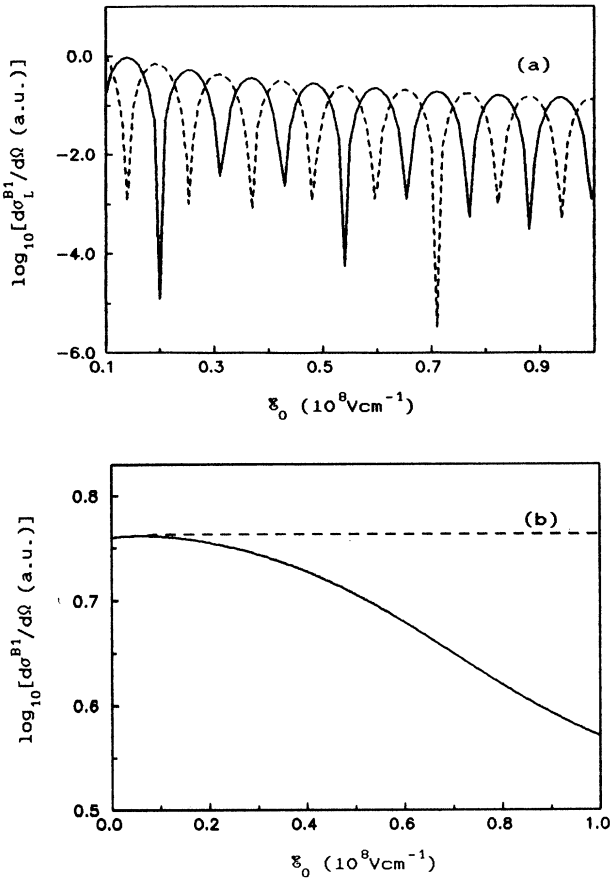

FIG. 8. The differential cross sections as functions of laser amplitude for $\mathcal{E}_0 \| \mathbf{k}_I$, $\theta = 10°$, $\hbar\omega = 1.0$ eV, $E_I = 50.0$ eV. (a) Individual cross sections. ——, $L = 0$; — — —, $L = 1$. (b) Summation cross section. ——, laser presented; — — —, laser free.

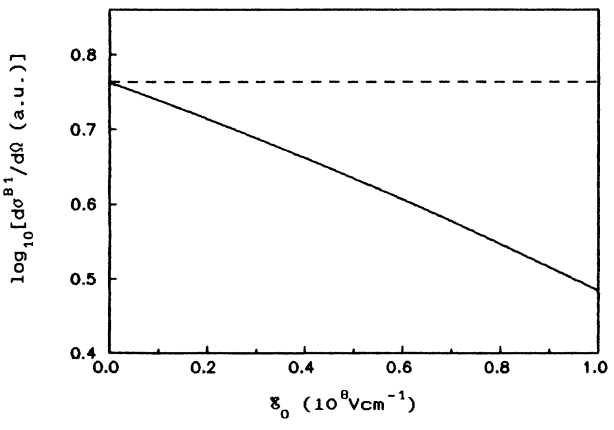

FIG. 9. Same as Fig. 8, but $\mathcal{E}_0 \perp \mathbf{k}_I$, $\theta = 10°$, $\varphi = 0°$.

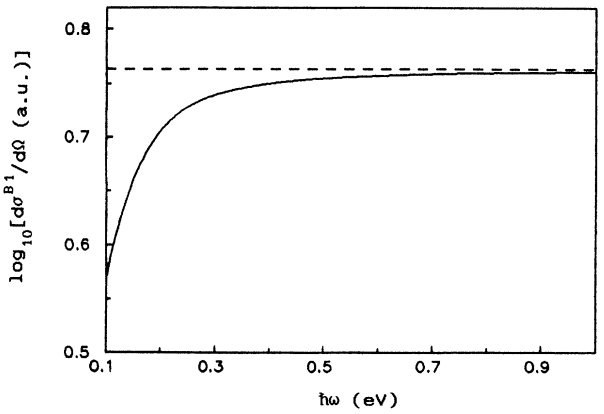

FIG. 10. The relation between differential cross section and laser frequency for $\mathcal{E}_0 \| \mathbf{k}_I$, $\theta = 10°$, $\mathcal{E}_0 = 1.0 \times 10^7$ V cm^{-1}, $E_I = 50.0$ eV. ——, laser presented; — — —, laser free.

atom but repels the positron, so there is a "hold-back effect" exerted on the Ps atom. When the horizontally polarized laser is presented, the Ps atom becomes "loose" along the Z direction. As the result, the "hold-back effect" is strengthened, and the Ps atom is slowed down. According to Eq. (3.2), the differential cross section will decrease at a small scattering angle. The principal contribution to the integral cross section comes from the small angular region, therefore the integral cross section decreases.

In Fig. 15, we illustrate the integral cross sections as functions of laser amplitude for $\hbar\omega = 1.0$ eV, $E_I = 50$ eV. Curve I represents the result for $\mathcal{E}_0 \| \mathbf{k}_I$, which is a decreasing function of $\mathcal{E}_0$; in contrast, curve II for $\mathcal{E}_0 \perp \mathbf{k}_I$ is an increasing function.

Figure 16 reveals the relation between the integral cross sections and laser frequency. The tendency for both geometries is also opposite. In Fig. 16(a) for $\mathcal{E}_0 \| \mathbf{k}_I$, the curve goes up; Fig. 16(b) for $\mathcal{E}_0 \perp \mathbf{k}_I$, the curve goes down. The latter is more sensitive.

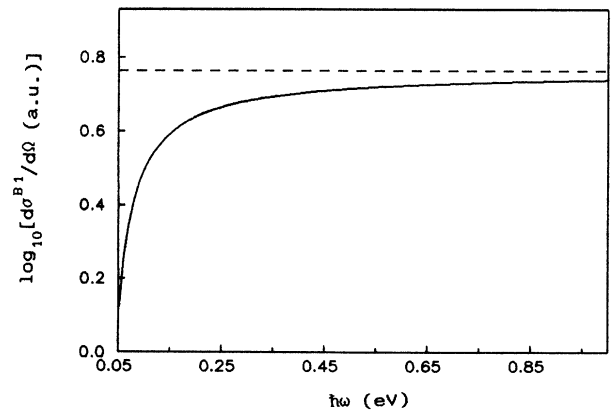

FIG. 11. Same as Fig. 10, but for $\mathcal{E}_0 \perp \mathbf{k}_I$, $\theta = 10°$, $\varphi = 0°$.

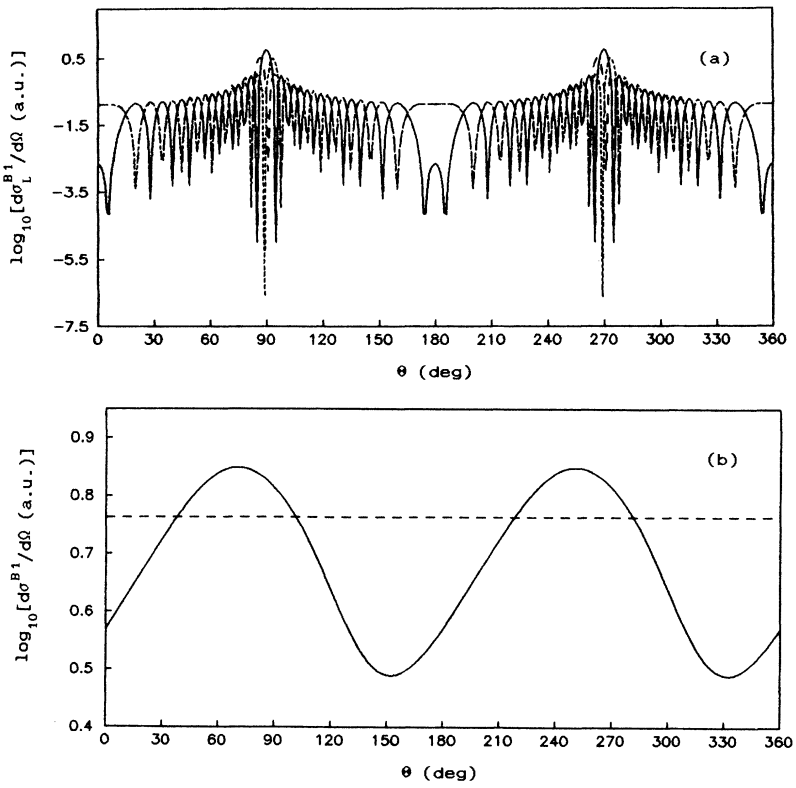

FIG. 12. The relation between the differential cross section and the laser polarized direction for $\theta=10°$, $\varphi=0°$, $\mathcal{E}_0=1.0\times10^7$ V cm^{-1}, $\hbar\omega=1.0$ eV, $E_I=50.0$ eV. (a) Individual cross sections. ——, $L=0$; — — —, $L=1$; ··· ··· ···, $L=-1$. (b) Summation cross section. ——, laser presented; — — —, laser free.

IV. CONCLUSION

In this work, we have extended our treatment of the laser-assisted binary rearrangement theory to the e^+-He collision, and have developed the exponential-parameter integration technique. This technique and the Feynman integration technique we employed in a preceding paper are very useful in solving the physical problems that involve these kinds of typical integrals.

Our results show substantial differences between the atomic hydrogen and helium target: For the atomic-hydrogen target, as has been studied in our preceding paper [5], the laser causes the integral cross section to increase. For the helium target though, the laser can either increase (when the laser electric vector is perpendicular to the incident positron momentum) or decrease (when the laser electric vector is parallel to positron momentum) the integral cross section for Ps formation. The main reason lies in the following fact: As for the atomic-hydrogen target, the nucleus binds the valence electron relatively loosely, which enables the laser at the strength considered to have a considerable dressing effect on it. This dressing effect loosens the target further, thereby promoting the probability of Ps formation. On the contrary, for the helium target, the electrons are bounded tightly by the nucleus. The dressing effect of the laser on

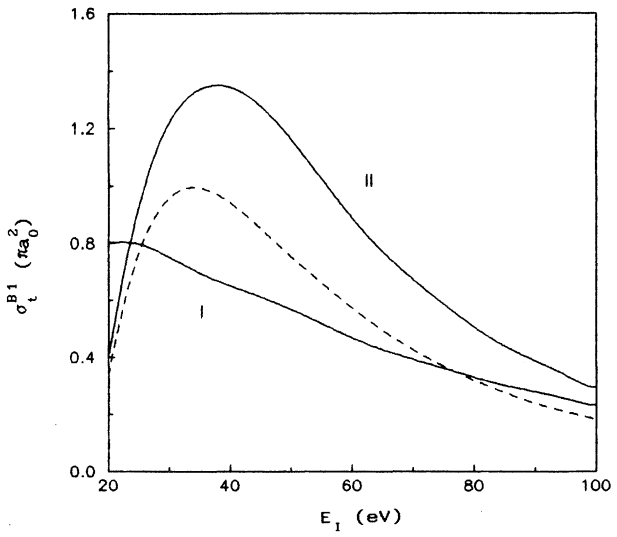

FIG. 13. Total cross sections for Ps formation in the e^+-He rearrangement collision for $\mathcal{E}_0=1.0\times10^8$ V cm^{-1}, $\hbar\omega=1.0$ eV. ——, I: $\mathcal{E}_0\|\mathbf{k}_I$; ——, II: $\mathcal{E}_0\perp\mathbf{k}_I$; — — —, laser free.

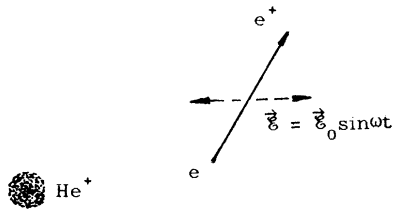

FIG. 14. The interaction between Ps and He^+.

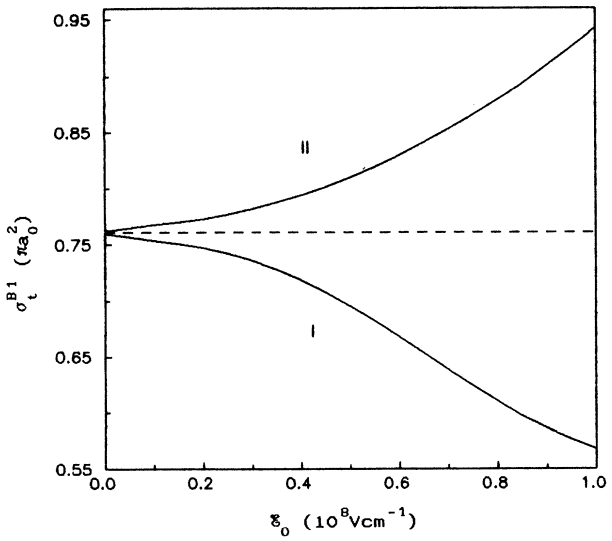

FIG. 15. The relation between total cross sections and laser amplitude for $\hbar\omega=1.0$ eV, $E_I=50.0$ eV. ——, I; $\mathcal{E}_0\|\mathbf{k}_I$; ——, II: $\mathcal{E}_0\perp\mathbf{k}_I$; — — —, laser free.

the target helium and helium ion can be neglected. Only the dressed effect of the Ps atom is important. As a result, when the electric vector is in the direction of incident momentum, the atomic core He^+ in the final channel exerts a "hold-back effect" on the polarized Ps atom, which lowers the probability of Ps formation. Hence the integral cross section is decreased.

Until now, there is no experimental result concerning the laser-assisted positron-atom rearrangement collisions reported. The main difficulty may result from the accessibility of the high-intensity laser and the measurement of positronium. In Fig. 17, for the case of laser-free cross sections, we give a comparison between our result and the results obtained by other authors [1,4]. To first Born approximation, our result is better than that gained by Ghosh, Mandel, and Sil [4]. Generally speaking, to test the theory, the experiment for helium target is easier to perform than that for atomic-hydrogen target, because the helium sample is easier to obtain and the theory-experiment comparison for helium should be better.

ACKNOWLEDGMENTS

It is a pleasure to thank Professor Liu Yao-Yang and Zhou Zi-Fang for their constructive suggestions. Mr. Sun Yi, Mr. Wang Bin, Mr. Kuang Ji-Yun, and Mr. Chen Xiao-Xi provided us with some expert help. We thank Dr. Murray Sherk for reading the manuscript. This work is supported by CRAAMD (Chinese Research for Atomic and Molecular Data) and the special foundation for doctoral training for the National Education Committee of China under Grant No. 9035805.

APPENDIX

In calculating the laser-assisted positron-helium rearrangement collision, we have to reduce another kind of integral which relates to the dressing effect of a laser. Its general form is

$$J(\mathbf{A},\alpha,\mathbf{B},\beta,\lambda)=\frac{1}{8\pi^2 i}\int d^3(r_1 r_2)\frac{e^{-i\mathbf{A}\cdot\mathbf{r}_1-\alpha r_1}}{r_1^2}\hat{\mathbf{e}}_z\cdot\hat{\mathbf{r}}_1 \times\frac{e^{-i\mathbf{B}\cdot\mathbf{r}_2-\beta r_2}}{r_2}\frac{e^{-\lambda r_{12}}}{r_{12}}, \quad \text{(A1)}$$

where $\mathbf{A}$, $\mathbf{B}$, α, β, and λ are parameters, $\hat{\mathbf{e}}_z$ and $\hat{\mathbf{r}}_1$ are the unit vectors in the direction of Z axis and $\mathbf{r}_1$, respectively, $r_{12}=|\mathbf{r}_1-\mathbf{r}_2|$. The integral (A1) cannot be reduced by Feynman's formula directly, because the integrand contains the factor $\hat{\mathbf{e}}_z\cdot\mathbf{r}_1$. As a treatment, one can expand each factor in the integrand into the series of the Bessel functions and the spherical harmonics, then reduce each

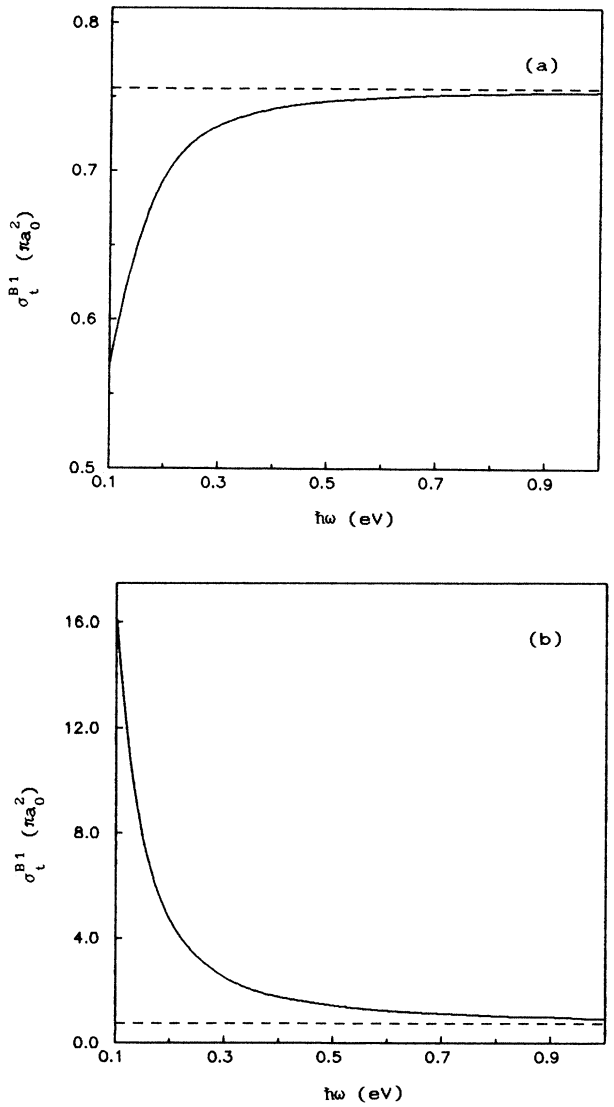

FIG. 16. Total cross sections as functions of laser frequency for $\mathcal{E}_0=1.0\times10^7$ V cm^{-1}, $E_I=50.0$ eV. ——, I: $\mathcal{E}_0\|\mathbf{k}_I$; ——, II: $\mathcal{E}_0\perp\mathbf{k}_I$; — — —, laser free.

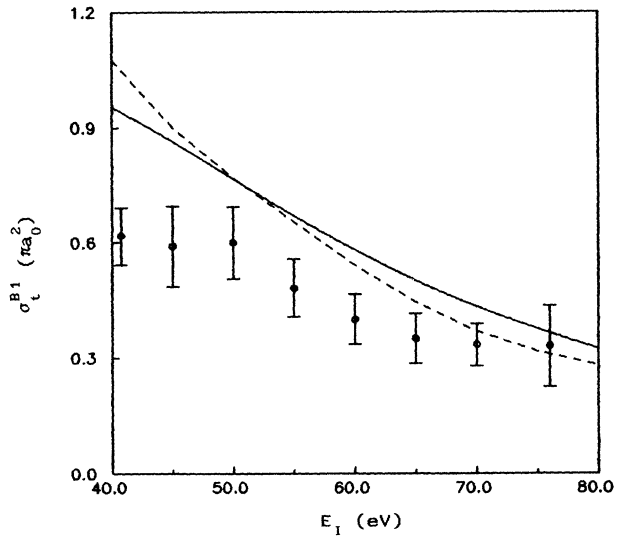

FIG. 17. The total cross sections for Ps formation in the absence of laser. ——, our result; — — —, FBA total cross section obtained by Mandal, Ghosh, ansd Sil; +, the experiment result of Fornari, Diana, Coleman.

term by using the formulas of the Bessel functions. But the reduction is too complicated. Here we adopt another treatment, the exponential-parameter integration technique.

Introducing the exponential-parameter integral

$$\frac{e^{-\alpha r_1}}{r_1}=\int_\alpha^\infty d\alpha' e^{-\alpha' r_1}, \tag{A2}$$

then substituting it into Eq. (A1), we obtain

$$J(\mathbf{A},\alpha,\mathbf{B},\beta,\lambda)=\frac{1}{8\pi^2 i}\int d^3r_2\frac{e^{-i\mathbf{B}\cdot\mathbf{r}_2-\beta r_2}}{r_2}\times\int d^3r_1\int_\alpha^\infty d\alpha'\frac{e^{-i\mathbf{A}\cdot\mathbf{r}_1-\alpha' r_1}}{r_1}\times\hat{\mathbf{e}}_z\cdot\hat{\mathbf{r}}_1\frac{e^{-\lambda r_{12}}}{r_{12}}. \tag{A3}$$

First, it is essential to show that the integrals $\int d^3r_1$ and $\int_\alpha^\infty d\alpha'$ in Eq. (A3) are exchangeable, i.e.,

$$\int d^2r_1\int_\alpha^\infty d\alpha' f(\alpha',\mathbf{r}_1,\mathbf{r}_2)=\int_\alpha^\infty d\alpha'\int d^2r_1 f(\alpha',\mathbf{r}_1,\mathbf{r}_2), \tag{A4}$$

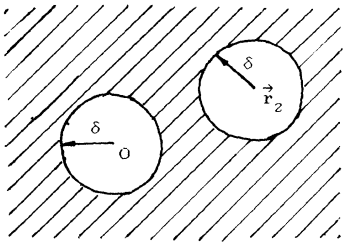

FIG. 18. $\mathbf{r}_1$ space.

where

$$f(\alpha',\mathbf{r}_1,\mathbf{r}_2)=\frac{e^{-i\mathbf{A}\cdot\mathbf{r}_1-\alpha' r_1}}{r_1}\hat{\mathbf{e}}_z\cdot\hat{\mathbf{r}}_1\frac{e^{-\lambda r_{12}}}{r_{12}}. \tag{A5}$$

To do this, we break the $\mathbf{r}_1$ space into three parts: $r_1<\delta$ ($\delta\to 0^+$), $|\mathbf{r}_1-\mathbf{r}_2|<\delta$, and the remaining closed set $\bar{V}$, as shown in Fig. 18. Within the spheroid $r_1<\delta$ we find

$$\int_{r_1<\delta}d^3r_1\int_\alpha^\infty d\alpha' f(\alpha',\mathbf{r}_1,\mathbf{r}_2)\approx 2\pi\int_0^\delta dr_1\int_0^\pi d\theta_1\sin\theta_1\cos\theta_1\frac{e^{-\lambda r_2}}{r_2}\approx 0. \tag{A6}$$

Similarly, in $|\mathbf{r}_1-\mathbf{r}_2|<\delta$, it is easy to show

$$\int_{|\mathbf{r}_1-\mathbf{r}_2|<\delta}d^3r_1\int_\alpha^\infty d\alpha' f(\alpha',\mathbf{r}_1,\mathbf{r}_2)\approx\frac{e^{-i\mathbf{A}\cdot\mathbf{r}_2-\alpha r_2}}{r_2^2}\hat{\mathbf{e}}_z\cdot\hat{\mathbf{r}}_2\int_{|\mathbf{r}_1-\mathbf{r}_2|<\delta}d^3r_1 r_1\approx 0. \tag{A7}$$

In the closed set $\bar{V}$, the integrand on the left-hand side of Eq. (A4) satisfies

$$\int_\alpha^\infty d\alpha' f(\alpha',\mathbf{r}_1,\mathbf{r}_2)=\left|\frac{e^{-i\mathbf{A}\cdot\mathbf{r}_1-\alpha r_1}}{r_1^2}\hat{\mathbf{e}}_z\cdot\hat{\mathbf{r}}_1\frac{e^{-\lambda r_{12}}}{r_{12}}\right|\le\frac{1}{r_1^2}\frac{1}{r_{12}}\le\frac{1}{\delta^2}\frac{1}{\delta}=\frac{1}{\delta^3}, \tag{A8}$$

therefore the integral $\int_\alpha^\infty d\alpha' f(\alpha',\mathbf{r}_1,\mathbf{r}_2)$ is convergent. According to the theorem for integration with respect to parameters [9], the integrals $\int_{\bar{V}}d^3r_1$ and $\int_\alpha^\infty d\alpha'$ should be exchangeable:

$$\int_{\bar{V}}d^3r_1\int_\alpha^\infty d\alpha' f(\alpha',\mathbf{r}_1,\mathbf{r}_2)=\int_\alpha^\infty d\alpha'\int_{\bar{V}}dr\,d^3r_1 f(\alpha',\mathbf{r}_1,\mathbf{r}_2). \tag{A9}$$

Summing up Eqs. (A6), (A7), and (A9), we obtain

$$\int dr_1^3\int_\alpha^\infty d\alpha' f(\alpha',\mathbf{r}_1,\mathbf{r}_2)=\left[\int_{r_1<\delta}+\int_{|\mathbf{r}_1-\mathbf{r}_2|<\delta}+\int_{\bar{V}}\right]d^3r_1\int_\alpha^\infty d\alpha' f(\alpha',\mathbf{r}_1,\mathbf{r}_2)=\int_{\bar{V}}d^3r_1\int_\alpha^\infty d\alpha' f(\alpha',\mathbf{r}_1,\mathbf{r}_2)=\int_\alpha^\infty d\alpha'\int_{\bar{V}}d^3r_1 f(\alpha',\mathbf{r}_1,\mathbf{r}_2)=\int_\alpha^\infty d\alpha'\int dr_1^3 f(\alpha',\mathbf{r}_1,\mathbf{r}_2). \tag{A10}$$

So far Eq. (A4) is proved.

Now we may evaluate the integral J. Substituting Eqs. (A4) and (A5) into Eq. (A3), we get

$$J(\mathbf{A},\alpha,\mathbf{B},\beta,\lambda)=\frac{1}{8\pi^2 i}\int_\alpha^\infty d\alpha'\int d^3r_2\frac{e^{-i\mathbf{B}\cdot\mathbf{r}_2-\beta r_2}}{r_2}\int d^3r_1\frac{e^{-i\mathbf{A}\cdot r_1-\alpha' r_1}}{r_1^2}\hat{\mathbf{e}}_z\cdot\mathbf{r}_1\frac{e^{-\lambda r_{12}}}{r_{12}}. \tag{A11}$$

Reusing the exponential integral (A2) and then exchanging the integral order, we obtain

$$\begin{aligned}J(\mathbf{A},\alpha,\mathbf{B},\beta,\lambda)&=\frac{1}{8\pi^2 i}\int_\alpha^\infty d\alpha'\int d^3r_2\frac{e^{-i\mathbf{B}\cdot\mathbf{r}_2-\beta r_2}}{r_2}\int d^3r_1\int_{\alpha'}^\infty d\alpha''\frac{e^{-i\mathbf{A}\cdot\mathbf{r}_1-\alpha'' r_1}}{r_1}\hat{\mathbf{e}}_z\cdot\mathbf{r}_1\frac{e^{-\lambda r_{12}}}{r_{12}}\\&=\int_\alpha^\infty d\alpha'\int_{\alpha'}^\infty d\alpha''\int d^3(r_1r_2)\frac{e^{-i\mathbf{B}\cdot\mathbf{r}_2-\beta r_2}}{r_2}\frac{e^{-i\mathbf{A}\cdot\mathbf{r}_1-\alpha'' r_1}}{r_1}\hat{\mathbf{e}}_z\cdot\mathbf{r}_1\frac{e^{-\lambda r_{12}}}{r_{12}}\\&=\int_\alpha^\infty d\alpha'\int_{\alpha'}^\infty d\alpha''\frac{\partial}{\partial A_z}I(\mathbf{A},\alpha'',\mathbf{B},\beta,\lambda),\end{aligned} \tag{A12}$$

where [5]

$$\begin{aligned}I(\mathbf{A},\alpha'',\mathbf{B},\beta,\lambda)&=\frac{1}{8\pi^2}\int d^3(r_1r_2)\frac{e^{-i\mathbf{A}\cdot\mathbf{r}_1-\alpha'' r_1}}{r_1}\frac{e^{-i\mathbf{B}\cdot\mathbf{r}_2-\beta r_2}}{r_2}\frac{e^{-\lambda r_{12}}}{r_{12}}\\&=\int_0^1 d\xi\frac{1}{\rho[(\rho+\alpha'')^2+q^2]},\end{aligned} \tag{A13}$$

with

$$\mathbf{q}=\mathbf{A}+\mathbf{B}\xi, \tag{A14}$$

$$\rho=[\lambda^2+(B^2+\beta^2-\lambda^2)\xi-B^2\xi^2]^{1/2}. \tag{A15}$$

Consequently, Eq. (A12) is written as

$$\begin{aligned}J(\mathbf{A},\alpha,\mathbf{B},\beta,\lambda)&=\int_\alpha^\infty d\alpha'\int_{\alpha'}^\infty d\alpha''\int_0^1 d\xi\frac{\partial}{\partial A_z}\frac{1}{\rho[(\rho+\alpha'')^2+q^2]}\\&=\int_0^1 d\xi\int_\alpha^\infty d\alpha'\int_{\alpha'}^\infty d\alpha''\frac{\partial}{\partial A_z}\frac{1}{\rho[(\rho+\alpha'')^2+q^2]}.\end{aligned} \tag{A16}$$

In Eq. (A16), the function

$$g(\xi,\alpha'')=\frac{1}{\rho[(\rho+\alpha'')^2+q^2]} \tag{A17}$$

satisfies the following conditions: (i) continuous and differentiable; the (ii) integral $\int_{\alpha'}^\infty d\alpha'' g(\alpha'',\xi)$ is convergent; and (iii) $\int_{\alpha'}^\infty d\alpha''[\partial/\partial A_z]g(\alpha',\xi)]$ is uniformly convergent. According to the theorem for differentiating an integral with respect to its parameter [9], we obtain

$$\int_{\alpha'}^\infty d\alpha''\frac{\partial}{\partial A_z}g(\alpha'',\xi)=\frac{\partial}{\partial A_z}\int_{\alpha'}^\infty d\alpha'' g(\alpha'',\xi). \tag{A18}$$

So Eq. (A16) my be written as

$$\begin{aligned}J(\mathbf{A},\alpha,\mathbf{B},\beta,\lambda)&=\int_0^1 d\xi\int_\alpha^\infty d\alpha'\frac{\partial}{\partial A_z}\int_\alpha^\infty d\alpha''\frac{1}{\rho[(\rho+\alpha'')^2+q^2]}\\&=\int_0^1 d\xi\int_\alpha^\infty d\alpha'\frac{\partial}{\partial A_z}\frac{1}{\rho q}\arctan\frac{q}{\alpha'+\rho}\\&=\int_0^1 d\xi\frac{1}{\rho}\frac{q_z}{q^3}\frac{\rho+\alpha}{\rho}\left[\frac{\pi}{2}-\arctan\frac{\rho+\alpha}{q}\right].\end{aligned} \tag{A19}$$

Here the following integration formulas [9] have been used:

$$\int dx\frac{1}{ax^2+c}=\frac{1}{\sqrt{ac}}\arctan(x\sqrt{a/c}), \tag{A20}$$

$$\int dx\arctan(ax)=x\arctan(ax)-\frac{1}{2a}\ln(1+a^2x^2). \tag{A21}$$

[1] L. S. Fornari, L. M. Diana, and P. G. Coleman, Phys. Rev. Lett. **51**, 2276 (1983).
[2] M. Charton, Rep. Prog. Phys. **48**, 737 (1986).
[3] H. S. W. Massey and A. H. Moussa, Proc. Phys. Soc. **77**, 811 (1961).
[4] P. Mandal, A. S. Ghosh, and N. C. Sil, J. Phys. B **8**, 2377 (1975).
[5] Li Shu-Min, Zhou Zi-Fang, Zhou Jian-Ge, and Liu Yao-Yang (unpublished).
[6] V. B. Berestetskiĭ, E. M. Lifshitz, and L. P. Pitaevskiĭ, *Recidivistic Quantum Theory* (Pergamon, London, 1971).
[7] C. J. Joachain, *Quantum Collision Theory* (North-Holland, Amsterdam, 1983).
[8] F. W. Byron, Jr., P. Francken, and C. J. Joachain, J. Phys. B **20**, 5487 (1987).
[9] *Mathematical Handbook* (Advanced Educational Publishing House, Beijing, 1979).